ISSN 1846-6168 (Print), ISSN 1848-5588 (Online)
https://doi.org/10.31803/tg-20240404220017

Preliminary communication
Received: 2024-04-04, Accepted: 2024-10-01

Experimental Investigation on Material Removal Rate and Tool Wear Rate for Machining Metal Matrix Composites in EDM Process

Abbas Fadhil Ibrahim*, Shakir M. Mousa, Semyan Omed Alyousifi, Diana Abed al Kareem Noori

Abstract: Electrical discharge machining (EDM) is one of non-traditional cutting method or manufacturing process for processing brittle and solid materials like composite materials and other difficult to machine materials. It is most usually utilized to manufacture metal matrix composites (MMCs) and is very solid materials. Aluminum based MMCs are to a large degree utilized in defense and aviation parts for their advanced and new characteristics like strength to weight ratio, high rigidity etc. The aluminum alloy 6061 and 7.5% SiC has been used as a workpiece and copper as a tool electrode, discharge current (I_p), pulse on-time (T_{on}), and pulse off-time (T_{off}) were selected as machining dependent variables for this study. The dependent variables were tool wear rate (*TWR*) and material removal rate (*MRR*). The experiments are planned using Box-Behnken design. Empirical models are developed for *MRR* and *TWR* using the analysis of variance (ANOVA) and regression models. The getted results showed that the *MRR* is increasing with increasing in I_p and T_{on} while *TWR* is decreasing when I_p and T_{on} is increase.

Keywords: analysis of variance; electrical discharge machining; material removal rate; tool wear rate

1 INTRODUCTION

In conventional machines, it is difficult to machining hardened and composite materials at high speed and acceptable surface quality. A non-conventional process, like (EDM), is the better choice for this kind of material to overcome these conditions [1]. Electrical discharge machining emerged for the manufacture of conductive materials that are hard or impossible to cut with conventional machines [2]. However, the primary cause of the EDM machining will be specified by electrical conditions like voltage, package current, pulse time length, workpiece material and characteristic of electrode, such as thermal conductivity and material melting temperature [3, 4]. Copper works well as a tool and is vastly used when smooth work-piece finishing are required [5]. As a result of the interest in the development of electrical discharge machines, this led to significant improvements in EDM technology. Currently, advanced electrical discharge machines are available for most applications of machine workshops [6]. Metal Matrix Compounds (MMCs) are relatively low density based on magnesium or, aluminum, or titanium and stiffeners such as Al_2O_3, SiC, TiB_2 or TiC [7, 8]. MMCs provides support and distributes the load to the structure while the particle or fiber stiffeners from supply useful mechanical, physical or thermal as performance. Therefore, MMCs are light metal or alloy and have high specific characteristics (like wear resistance, toughness, and strength), becoming a sought-after alternative in industrial applications. MMCs are produced in many different manufacturing process (like molding Metal injection, friction stirring process, mechanical alloying, pressure casting technology, continuous binder powder coating, etc.) [9]. Silicon carbide (SiC), which is also famous as carborundum, has very good mechanical characteristics. And thermal conductivity the value of the density of Silicon carbide is similar to that of Al. Therefore SiC reinforcement alloy composites are the typical choosing of material for defends functionalities in flight, defense purposes, rigged structural, and heavy manufacturing industries, owing to their tribological and mechanical properties [10].

Several experiments and investigations conducted in the EDM process, it was observed that the melting points is impact to the *TWR* and the *MRR* increased with increasing I_p. Ref. [11] investigated the effect of controllable parameters of I_p, V, and pulse duration and duty cycle on process response such as *TWR*, *MRR* and *Ra* with cry therapy electrode. The results show that I_p and T_{on} and duty cycles have an important influence on the TWR and MRR. Ref. [12] examined T_{on} and I_p in Inconel 718 EDM with a CuW as a tool. The values indicated that the maximum removal rate was 28.37 mm^3/min with highest I_p (40 A) and longest tone (400 µs). Ref. [1] studied optimization of variables for silicon zed silicon carbide (SiSiC) on the responses; *TWR*, *Ra* and *MRR*. By new design (FCCC) was utilized on the experiments [13]. The work studied the topical surface property of an arranged Titanium (Ti-6Al-4V) alloys in (EDM) process. Ref. [14] prepared the metal matrix composite, AA 6061 reinforced with 5wt% SiC particles by stir casting method, in EDM machining process to determine MRR and SR. Ref. [15] discussed the experiments of the EDM that were conducted to examine the influence of machining parameters, including current, pulse on, and duty factors on the MRR, and SR of the Al-alloy with-5%SiC-10%B4C hybrid composite as workpiece using copper electrode tool by Box-Behnken design. Ref. [16] Conducted a hybrid magnetic field assisted powder mixed on silicon carbide (Al-SiC) MMCs, current, P_{on} and P_{off} affected the duration and type of dielectric conditions significantly on the removal rate. The electrical energy in EDM is changed to heat energy by the series of separate electrical discharges that happen between the specimen and the electrode immersed in the dielectric medium, which works on this chain to melt then evaporate the metal from the workpiece surface, thus removing the material [17, 18].

The importance of the research lies in the manufacture and operation of Al alloy (6061) reinforced with 7.5% silicon carbide, has been fabricated through stir casting, which is characterized by high wear resistance, stiffness, and lightweight and can be used in molds, automobile industry, and nuclear plants.

In this paper, a composite material was employed as Al-alloy with 7.5% SiC reinforcement, current, pulse on duration, and pulse off duration were chosen as process parameters, while the material removal rate and the tool wear ratio were chosen as process performance indicators.

2 DETERMINE THE MATERIAL REMOVAL RATE AND TOOL WEAR RATE

Material removal rate is a performance measure of workpiece wear rate expressed in the volume of material separated from the sample per unit time and is usually used to determine the speed at which processing is performed. Melting point is a significant parameter in determining the wear of the tool and depends on the factors of the machine [19, 20]. *MRR* and *TWR* are determined in Eq. (1) and (2) respectively, which depend on the weight of the work piece and tool before and after manufacturing, as well as the processing time [21-23].

$$MRR = \frac{(W_b - W_a)\cdot 1000}{(\rho_w \cdot T_m)},\ \mathrm{mm}^3/\mathrm{min} \tag{1}$$

Where: W_b - weight of specimen before EDM (g), W_a - weight of specimen after EDM (g), T_m - processing time (min), ρ_w - density of specimen material (ρ_w = 2.77 g/cm^3).

$$TWR = \frac{(T_b - T_a)\cdot 1000}{(\rho_t \cdot T_m)},\ \mathrm{mm}^3/\mathrm{min} \tag{2}$$

Where: T_b - weight of tool before EDM (g), T_a - weight of tool after EDM (g), T_m - processing time (min), ρ_t - density of tool material (ρ_t = 8.96 g/cm^3).

3 METHODOLGY OF BOX–BEHNKEN DESIGN

Box–Behnken designs are experimental designs for response surface methodology used in various statistical operations, invented by George E. B. Box and Donald Behnken in 1960, where at least three levels are required to achieve the goal, where each independent variable is set to one of the three values and equally, usually coded as −1, 0, +1.

The Box–Behnken design is considered more efficient and reliable than other designs such as the central component design, the three-level full factor design, and the Dohlert design [24].

4 EXPERIMENTAL WORK

The composite material specimen is produced of an Al-alloy matrix (AA6061) and 7.5% SiC. Silicon carbide has been utilized as a good abrasive material and has been in products with grinding wheels for over a hundred years. After that, the material has been advanced into high-quality ceramics with thermal and high mechanical properties. It is utilized in many more applications. The material can also be made electrically conductive and highly resistant to heating. The stir-casting method was utilized to manufacture size material. The composite porosity is about 7.5% SiC reinforced with 50 µm as grain size. The experiment was planned design and survey analyzed by utilizing Minitab 19 software with 13 test according to Box-Behnken design. As well, input three parameters containing the I_p, T_{on}, and the T_{off} were selected for the investigation. The aluminum alloy was heated for one hour and the silicon carbide granules were melted at (750°C) to separate gases and moisture from the surface of the workpiece layer [9]. The preheated SiC particle powder was added (7.5%) into the melt metal. After adding the nano silicon carbide powder, and for the purpose of obtaining a better homogeneity and distribution, we continue to stir for 10 minutes. The molten state was kept for one minute to remove the slag. and then the molten aluminum was poured into the graphite moulds. The important properties of the matrix and reinforcement are shown in Tab. 1.

Table 1 Properties of AA6061 and SiC

Material	Density (kg/m^3)	Melting point (K)	Modulus of elasticity (MPa)	Thermal conductivity (W/m·K)
AA6061	2710	893	70000	180
SiC	3200	3003	410000	120

The experimental have been done on EDM machine (CM 323C) with kerosene as dielectric solution, as shown in Fig. 1.

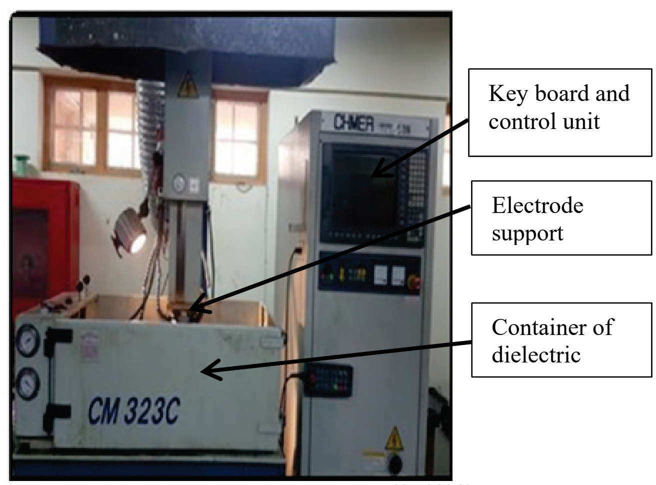

Figure 1 EDM type machine (CM323C)

In the experimental work a tool electrode was selected from pure copper material (∅4×100 mm). Copper has good EDM wear and better conductivity. The chemical composition for tool and AA6061 as shown in Tabs. 2 and 3 respectively.

Table 2 The chemical composition of Cu tool electrode W%

Pb	Sn	Si	Sb	Te	Cu
<0.005	0.003	0.010	0.033	0.015	Rem

Table 3 The chemical composition of specimen AA6061 W%

Cu	Mg	Si	Cr	Fe	Mn	Al
0.25	0.92	0.62	0.22	0.23	0.03	Rem

The normal workpiece polarity (+) was chosen. The study work includes thirteen tests according to the design of experiments and testing research plan. The machining parameters were listed in Tab. 4. It was selected based on previous research, which gives the best results for material removal rate and tool wear rate.

Table 4 Variables value

Variables	Symbol	Value		
		1	2	3
Current (A)	I_p	10	20	30
Pulse on duration (μs)	T_{on}	100	150	200
Pulse off duration (μs)	T_{off}	6	12	24

5 RESULTS AND DISCUSSION

According to the set of experimental outcomes achieved from Tab. 5 in appendix A, the influence of the independent variables P_i, T_{on} and T_{off} on the two dependent variables that is *MRR* and *TWR* by used copper tool. The (AA 6061) with 7.5 % SiC can easily be machined by electrical discharge machining and maximum material removal rate, minimum tool wear rate can be obtained by controlling the machining parameters. ANOVA and from MINITAB 19 software is utilized to determine the effective of variables on the desired achievement measures. The largest material removal rate occurred in experiment 11, where I_p (30 A), P_{on} (200 μs), and P_{off} (12 μs), this is due to the increase in current with the increase in pulse time, which will lead to an increase in the strength of the electric spark in the cutting zone and the melting of the material more quickly. While minimum tool wear rate occurred in experiment 2, where I_p (10A), P_{on} (100 μs), and P_{off} (12 μs), this is due to reducing the current value and pulse time, which leads to increasing the tool life.

Table 5 Response (output) result and Box–Behnken design of the set experiments

Run order	Current (A)	Pulse on (μs)	Pulse off (μs)	*MRR* measured (mm^3/min)	*MRR* predicted (mm^3/min)	*TWR* measured (mm^3/min)	*TWR* predicted (mm^3/min)
1	30	100	6	4.368	4.81705	0.6320	0.63131
2	10	100	12	2.521	2.98170	0.0290	0.09782
3	10	150	6	2.975	3.13805	0.1471	0.17733
4	20	150	12	4.814	4.73200	0.5580	0.54400
5	10	200	6	3.624	3.48575	0.1950	0.22353
6	30	200	6	5.517	5.51245	0.7630	0.72371
7	20	100	6	4.273	3.80370	0.5860	0.53111
8	10	200	24	2.362	2.56025	0.2640	0.15691
9	30	150	24	5.263	5.79625	0.5640	0.61089
10	20	200	24	4.336	4.35210	0.4880	0.55689
11	30	200	12	6.861	6.48230	0.6730	0.69040
12	30	100	24	5.780	5.44855	0.5890	0.56469
13	10	100	24	2.281	1.86485	0.0850	0.06451

5.1 Analysis of Variance (ANOVA)

The claimant's null hypothesis was used in response to the 95% confidence point and the specified effective boundary conditions are a partial quadratic model of the automated processing process. Fisher's test (F-test) the significance of the strong function. If the (p-value) is 0.05, it is concluded that this parameter has a statistically significant influence. Tabs. 6, and 7 referred to the definitions of information of ANOVA for the *MRR* and *TWR* of EDM process. From nonlinear regression models mathematical relationships were obtained between machining parameters, *MRR* and *TWR* as in Eqs. (3) and (4) respectively.

5.2 Prediction Mathematical Model of *MRR*

In order to estimate the final results of the *MRR* output response shown in Tab. (4), the ANOVA functions are run to decrease the p-value by utilizing the three-factor levels of the backward transform model. A model F value of 22.54 indicates that the pattern is significant. "Prob > F" values less than 0.05 referred the momentousness of the model terminology. Therefore, *current*, *pulse on time*, and the interaction between *current* and *pulse off time* are significant sample terms. The predicted regression model empirical equation for *MRR* is:

$$MRR = 0.487 + 0.0754 \cdot I_p + 0.00695 \cdot T_{on} + 0.148 \cdot T_{off} - \\ -0.00808 \cdot T_{off}^2 + 0.00432 \cdot I_p \cdot T_{off},\ \mathrm{mm^3/min} \tag{3}$$

Table 6 ANOVA for *MRR*

Source	DF	Sum of squares	Mean of squares	F-value	p-value
Model	5	23.1353	4.6271	22.54	0.000
Linear	3	20.9358	6.9786	34.00	0.000
A	1	19.6729	19.6729	95.84	0.000
B	1	1.2090	1.2090	5.89	0.046
C	1	0.0540	0.0540	0.26	0.624
Square	1	0.9873	0.9873	4.81	0.064
B×*B*	1	0.9873	0.9873	4.81	0.064
2-way int.	1	1.2121	1.2121	5.90	0.045
A×*C*	1	1.2121	1.2121	5.90	0.045
Error	7	1.4369	0.2053	/	/
Total	12	24.5723	/	/	/

The three-dimensional graphs presented in Figs. 2-4 were utilized to estimate and explicate the experimental model.

Fig. 2 shows that the (MR) increases with increasing I_p (up to 30 A) and the pulses over the duration (up to 200 µs) reach the value (6.861 mm^3/min), Presence of SiC particles affects higher *MRR* can be achieved by increasing current. Fig. 3 clarifies the 3D graphs for material removal rate (*MRR*) utilizing the I_p (30 A) and T_{off} (15 µs), and the maximum surface roughness obtained when using reaches, the values (6.861 mm^3/min). Fig. 4 shows the 3D graphs for *MRR* utilizing the T_{on} (200) and T_{off} (15 µs, and the last maximum (*MRR*) getted when utilizing the kerosene dielectric reaches the values (6.861 mm^3/min). This means that with get increasing the value of both the I_p and the T_{on}, the productivity increases. Thus, the T_{his} means that by get increasing the value of both the I_p and the T_{on}, productivity get increases. Thus, the amount of heat energy generated will be large, which leads to an increase in the melting process and successive abrasive to separate the out layers from the surface of the work piece.

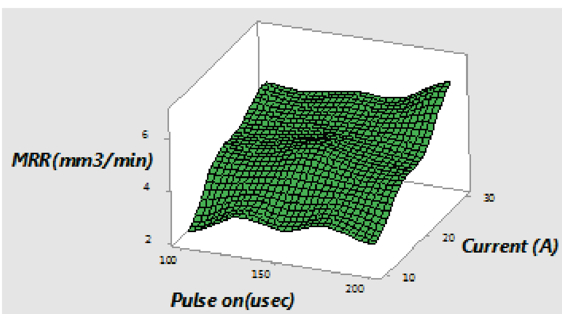

Figure 2 Relationship between *MR*R, current, and pulse on

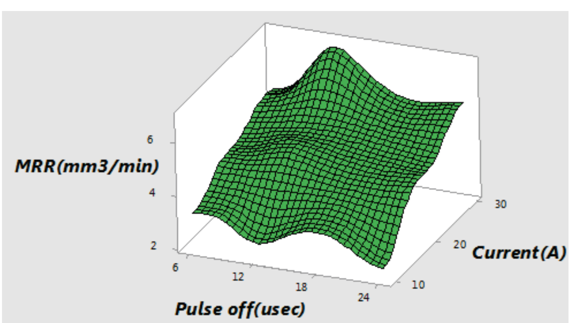

Figure 3 Relationship between *MRR*, pulse off, and current

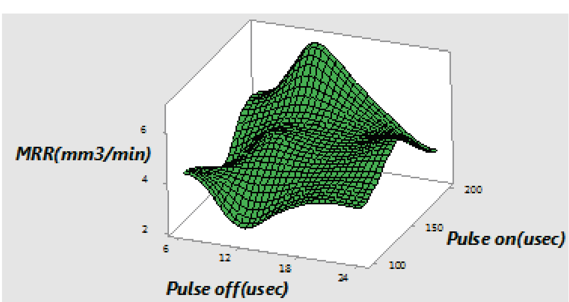

Figure 4 Relationship between *MRR*, pulse off, and pulse on

5.3 Prediction Mathematical Model of *TWR*

To evaluate the results of the instrument wear rate (*TWR*) given in Tab. 7 where the model F-value of 45.87 indicates that the model is significant. Therefore, *current*, *pulse on time*, and (*current*)^2 are very important specimen terms. The predicted final empirical equation is:

$$TWR = -0.639 + 0.085 \cdot I_p + 0.000924 \cdot T_{on} - \\ -0.0037 \cdot T_{off} - 0.001499 \cdot I_p^2,\ \text{mm}^3/\text{min} \quad (4)$$

In Eqs. (3) and (4) it was also apparent that the greatest significant machining variable input was current amplitude and impact on estimated or predicted *MRR* and then *TWR*

Table 7 ANOVA for *TWR*

Source	DF	Sum of squares	Mean of squares	F-value	p-value
Model	4	0.70974	0.177434	45.87	0.000
Linear	3	0.65789	0.219297	56.70	0.000
A	1	0.62545	0.625450	161.70	0.000
B	1	0.02134	0.021344	5.52	0.047
C	1	0.01110	0.011096	2.87	0.129
Square	1	0.05185	0.051847	13.40	0.006
A×*A*	1	0.05185	0.051847	13.40	0.006
Error	8	0.03094	0.003868	/	/
Total	12	0.74068	/	/	/

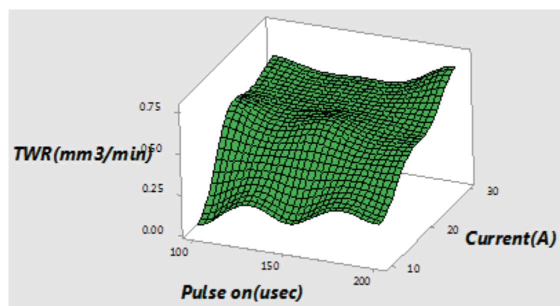

Figure 5 Relationship between *TWR*, current, and pulse on

Figs. 5-7 show the effect of the EDM variables on the *TWR*. Fig. 5 illustrates that when utilizing the I_p (10 A) and T_{on} (100 µs), the value of *TWR* decreased to (0.0290 mm^3/min). Fig. 6 indicates the 3D graphs for *TWR* using the pulse current (10 A) and pulse off duration (15 µsec), and the minimum *TWR* gets when utilizing reaches, the rate values (0.0290 mm^3/min). Fig. 7 shows the 3D graphs for *TWR* utilizing the I_p (100) and T_{on} (15 µsec), and the minimum value of *TWR* is reached (0.0290 mm^3/min).

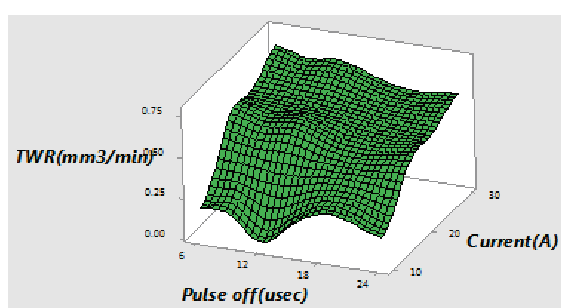

Figure 6 Relationship between material removal rates, current, and pulse off

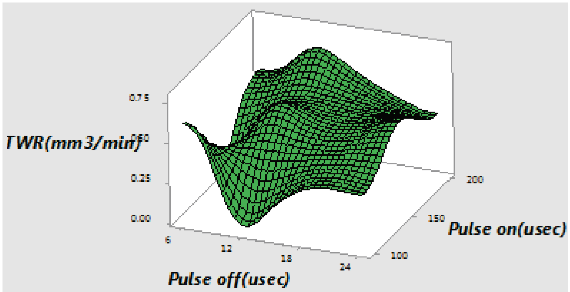

Figure 7 Relationship between material removal rates, pulse on, and pulse off

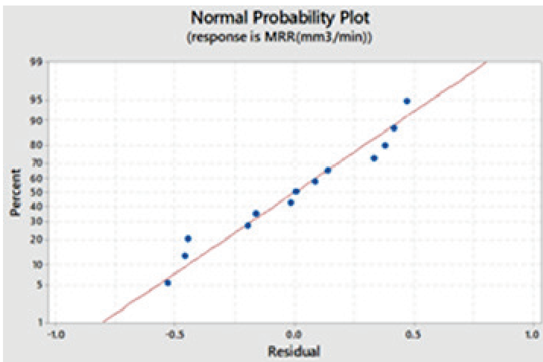

Figure 8 Probability plot for *MRR*

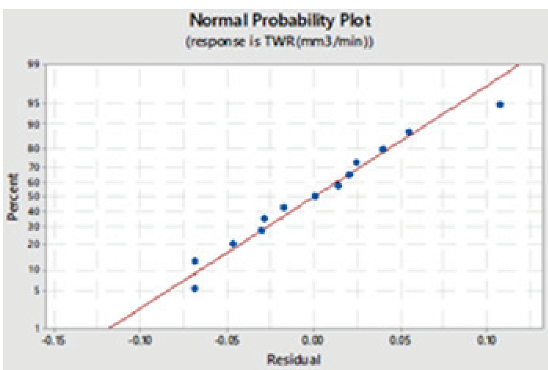

Figure 9 Probability plot for *TWR*

5.4 Probability plot for *MRR* and *TWR*

Figs. 8 and 9 are represents the normal plot of residuals for material removal rate and tool wear rate separately respectively. All data are clearly normal and there is no deflection from the usually, due all the points on the normal plot represented as in straight line.

5.5 SEM Inspection of Machined Surface

From Figs. 10 and 11 show the microstructure inspection for experiment 2 and 11 at the low and high energy respectively , where the processing input parameters in Fig. 10 are at pulse on time (100 µs), current (10 A) and pulse off time (12 µs). During the time that the processing input parameters in Fig. 11 at pulse time (200 µs), current (30 A) and pulse off time (12 µs), which showed in the state of a large quantity of highly molten material on the top layers' surface and very deep holes as well as micro-cracks.

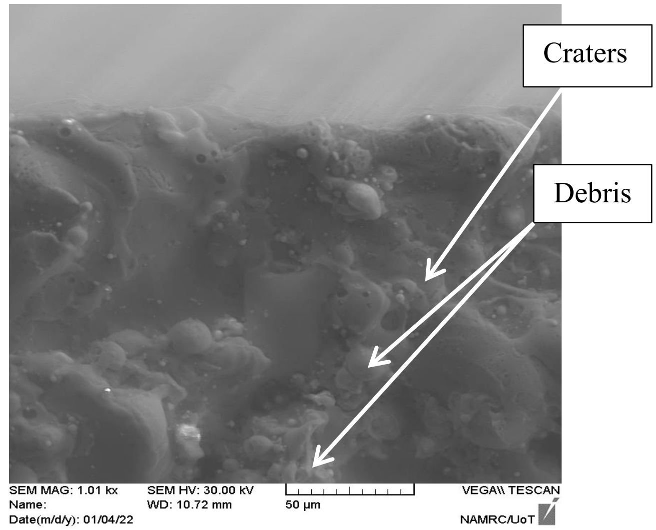

Figure 10 Fine structure microstructure of the machined surface at the low energy

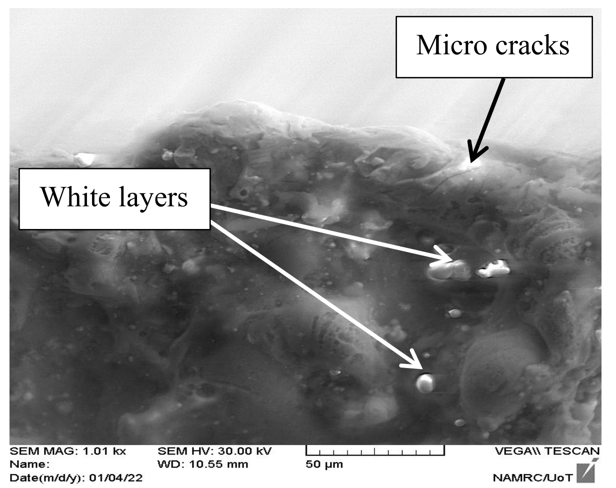

Figure 11 Fine structure microstructure of the machined surface at the high energy

Through the pulse on time value increases with time, more amount pulse discharge energy is released, thus generating more heat, resulting in the evaporation and melting of material a minute particles from the top surface of the workpiece and the action of forming relatively great large dark holes on the top surface. The still-remaining a thin piece of material sticks to the surface to form spherical pieces of waste as pellets and debris. When the particles of carbon react with the molten metal, it naturally and after that, the cooling process leads to union bonds greater than the original element, and when the stress on the surface exceeds the end the ultimate tensile strength of the material, in this case, cracks form.

6 CONCLUSIONS

In this study, has been made to estimate or predict (*TWR*) and (*MRR*) in EDM of Al-alloy with 7.5% SiC using a Box-Behnken design procedure. The maximum *MRR* is achieved when the I_p and T_{on} are very high and T_{off} is (12 µsec), whereas the lower value of *TWR* is observed when the I_p and T_{on} are minimum value and the T_{off} is 12 µs. ANOVA table shows that I_p and T_{on} are an important parameter. The normal probability plot indicates that the mathematical regression model agrees passably well with noticed values and the errors are normally distributed. In the next work, the study can be involved for other output responses like recast layer white (*RLW*), surface roughness (*SR*), and radial over cut (*ROC*). The final results from this paper will be beneficial for production engineers to choosing suitable design of process variable parameters to machine Al-alloy with 7.5% SiC.

7 REFERENCES

[1] Abdul Azeez, A., Jafri, M., Ahmad, M. & Hamidon M. (2017). Optimization of electrical discharge machining parameters of SiSiC through response surface methodology. *Journal Teknologi*, 79, 119-129. https://doi.org/10.11113/jt.v79.7622

[2] Ritesh Kumar, S., Sanjiv Kumar, T., Sharad Chandra, S. & Binay K. (2023). Hybrid Taguchi-GRA-CRITIC Optimization Method for Multi-Response Optimization of Micro-EDM Drilling Process Parameters. *Tehnicki Vjesnik,* 30(3), 804-814. https://doi.org/10.17559/TV-20220601114015

[3] Bhaskar, C., Jatinder, K. & Hari, S. (2017). Investigations into electrical discharge machining of fabricated AA 6061/10% Al_2O_3 aluminium-based metal matrix composite using OFAT approach. *Int. J. Automotive Composites*, 3, 29-43. https://doi.org/10.1504/IJAUTOC.2017.086514

[4] Gore, A. S. & Patil N. G. (2018). Wire electro discharge machining of metal matrix composites: A review. *Procedia Manufacturing*, 20, 41-52. https://doi.org/10.1016/j.promfg.2018.02.006

[5] Jawahir, I. S., Brinksmeier, E. & M'Saoub, R. (2011). Surface integrity in material removal processes: Recent advances. *Manufacturing Technology*, 60, 603-62. https://doi.org/10.1016/j.cirp.2011.05.002

[6] Arvinder, S. C., Harminder, S. B., Jasmaninder, S. G., Vettivel, S. C. & Raman, K. (2023). Tool wear rate during electrical discharge machining for aluminium metal matrix composite prepared by squeeze casting: A prospect as a biomaterial. *J. Electrochem. Sci. Eng., 13*(1), 149-162. https://doi.org/10.5599/jese.1391

[7] Abbas, F. I. (2022). Evaluation of surface roughness and material removal rate in electrical discharge machining of Al-alloy with 10% SiC. *IIUM Engineering Journal, 23*(1), 349-357. https://doi.org/10.31436/iiumej.v23i1.2114

[8] Liao, Z., Abdelhafeez, A., Li, H., Yang, Y., Diaza, O. G. & Axinte, D. (2019). State-of-the-art of surface integrity in machining of metal matrix composites. *Int. J. Mach Tool Manu.*, 143, 63-91. https://doi.org/10.1016/j.ijmachtools.05.006

[9] Mohammad, H., Muhammad, I. P. & Mukhtiar, A. U. (2011). Manufacturing of Aluminum Composite Material Using Stir Casting Process. *Mehran University Research Journal of Engineering & Technology*, 30, 37-40. https://doi.org/10.48550/arXiv.1604.01251

[10] Hadi, M. H. & Abbas, F. I. (2023). Experimental Study of Tool Wear Rate and Surface Roughness in Electrical Discharge Machining of Monel Alloy Using Cu-Gr Composite Electrode. *AIP Conference Proceedings, 2830*(1), 030009. https://doi.org/10.1063/5.0156914

[11] Hadi, M. H. & Abbas, F. I. (2022). Effect of Copper-Graphite Composite Electrode on Material Removal Rate and Surface Roughness in Monel 400 during Electrical Discharge Machining. *Metallurgical and Materials Engineering, 28*(2), 245-255. https://doi.org/10.30544/817

[12] Sengottuvel, P., Satishkumar, S. & Dinakaran, D. (2013). Optimization of Multiple Characteristics of EDM Parameters Based on Desirability Approach and Fuzzy Modeling. *Procedia Engineering*, 64, 1069-1078. https://doi.org/10.1016/j.proeng.2013.09.185

[13] Sulaiman, A., Ahsan, A. & Mohamed, K. (2018). Analysis of microlayer defects of a functionally graded titanium alloy by electrical discharge machining. *Engineering and Applied Science Research*, 45, 17-22. https://doi.org/10.14456/easr.2018.1

[14] Abbas, F. I., Shakir, M. M. & Diana, A. N. (2022). Investigation and optimization of machining parameters in electrochemical machining of aluminium metal matrix composites. *Periodicals of Engineering and Natural Sciences, 10*(3), 48-59.

[15] Abbas F. I., Abdullah H. S., al Kareem Noori, D. A. (2022). Investigation of material removal rate and surface roughness during electrical discharge machining on Al(6061)-5%SiC-10%B4C hybrid composite. *Metallurgical and Materials Engineering, 28 (1) p. 47-60*. https://doi.org/10.30544/798

[16] Rizovich Ablyaz, T., Singh Bains, P., Singh Sidhu, S., Ravilevich Muratov, K. & Sergeevich Shlykov, E. (2021). Impact of Magnetic Field Environment on the EDM Performance of Al-SiC Metal Matrix Composite. *Micromachines*. 12, 2-13. https://doi.org/10.3390/mi12050469

[17] Skoczypiec, S., Machno, M. & Bizon, W. (2015). The Capabilities of Electrodischarge Microdrilling of High Aspect Ratio Holes in Ceramic Materials. *Management and Production Engineering Review*, 6, 61-69. https://doi.org/10.1515/mper-2015-0027

[18] Sonawane, S. A. & Kulkarni, M. L. (2018). Multi Response Optimization of Wire Electrical Discharge Machining for Titanium Grade-5 by Weighted Principal Component Analysis. *International Journal of Engineering and Technology Innovation, 8*, 133-145.

[19] Srivastava, V. & Pandey, P. (2013). Experimental Investigation on EDM process with ultrasonic assisted cryogenically cooled electrode. *Journal of Engineering Manufacturing*, 227, 301-314.

[20] Munmun, B. & Kalipada, M. (2020). Effect of Powder Concentration on the EDM Performance of AISI 304 Using Cryotreated Post Tempered Electrodes. *Engineering Review*, 77-78. https://doi.org/10.30765/er.1655

[21] Sultan, T., Kumar, A. & Gupta, R. D. (2016). Material Removal Rate, Electrode Wear Rate, and Surface Roughness Evaluation in Die Sinking EDM with Hollow Tool through Response Surface Methodology. *Int. J. Manuf. Eng., 2014*, 1-16. https://doi.org/10.1155/2014/259129

[22] Uthayakumar, M., Thirumalai Kumaran, S., Adam Khan, M., Skoczypiec, S. & Bizon, W. (2020). Microdrilling of AA (6351)-SiC-B4C Composite Using Hybrid Micro-ECDM Process. *ASTM International. J. Test. Eval., 48*(4), 3073-3086. https://doi.org/10.1520/JTE20180216

[23] Abbas, F. I. (2021). Influence of electrical discharge machining parameters by additives Nano [AL_2O_3] on surface roughness and material removal rate in machining of AISI 304. *Journal of Physics: Conference Series*. https://doi.org/10.1088/1742-6596/1973/1/012154

[24] Karmoker, J. R., Hasan, I., Ahmed, N., Saifuddin, M. & Reza, M. S. (2019). Development and Optimization of Acyclovir Loaded Mucoadhesive Microspheres by Box-Behnken Design. *Dhaka University Journal of Pharmaceutical Sciences, 18*(1), 1-12. https://doi.org/10.3329/dujps.v18i1.41421

Authors' contacts:

Abbas Fadhil Ibrahim
(Corresponding author)
Production Engineering and Metallurgy,
University of Technology,
Baghdad, Iraq
E-mail: abbas.f.ibrahim@uotechnology.edu.iq

Shakir M. Mousa
Al-Furat Al-Awsat Technical University,
Technical Institute of Al-Mussaib, Babylon, Iraq

Semyan Omed Alyousifi
Manufacturing Department, Duhok Technical Institute,
Zakho Way Road, Duhok, Iraq

Diana Abed al Kareem Noori
Production Engineering and Metallurgy,
University of Technology,
Baghdad, Iraq